

# Adaptation of inorganic quantum dots for stable molecular beacons

Joong Hyun Kim<sup>a</sup>, Dimitrios Morikis<sup>a</sup>, Mihrimah Ozkan<sup>a,b,\*</sup>

<sup>a</sup> Department of Chemical and Environmental Engineering, University of California Riverside, Riverside, CA 92521, USA

<sup>b</sup> Department of Electrical Engineering, University of California Riverside, A241 Bourns Hall, Riverside, CA 92521, USA

Received 22 June 2003; accepted 22 April 2004

Available online 10 June 2004

## Abstract

We have developed semiconductor quantum dots (QDs)-conjugated molecular beacons (MBs). The organic fluorophores are replaced with inorganic fluorescent ZnS-capped CdSe quantum dots covered with mercaptoacetic acid monolayer. We confirmed the overlap between emission spectrum of the QD after the surface modification and the absorption spectrum of 4-(4'-dimethylaminophenylazo) benzoic acid (DABCYL) as an organic quencher molecule. About 90% overlap between QDs and DABCYLs' spectra promotes fluorescent resonance energy transfer (FRET). FRET efficiency between QD-DABCYL and 6-FAM (organic fluorophore)-DABCYL are compared by using 3-D molecular modeling. The farthest and nearest possible separation between the fluorophore and the quencher are predicted using 3-D molecular model considering the rotational freedom of the bonds defined by the type of chemical linker between MB-fluorophore and MB-DABCYL. Finally, QD-modified MBs are tested with their complementary target deoxyribonucleic acid (DNA) sequence and for non-specific sequences. The use of QDs instead of organic fluorophores may offer multiplexed imaging during DNA or RNA analysis due to their broad UV absorption spectrum.

© 2004 Elsevier B.V. All rights reserved.

**Keywords:** Semiconductor quantum dot; Molecular beacon; DABCYL

## 1. Introduction

Molecular beacons (MBs) have been developed by Tyagi and Kramer [1] in 1996. The first MB consisted of 5-base pairs of stem section and 18-bases loop section which is complementary to a desired target nucleic acid sequence. In addition, 5' end was attached to 5-(2'-aminoethyl) aminonaphthalene-1-sulfonic acid (EDNS), fluorophore and 3' end was attached to a 4-(4'-dimethylaminophenylazo) benzoic acid (DABCYL), quencher molecule. In the absence of the target DNA sequence, by Watson–Crick hybridization of complementary sequences of the stem section, MBs form hairpin structure in which the fluorophores and quenchers are in close proximity that energy from fluorophores is transferred to the quencher molecules. As a result, this energy is absorbed by the DABCYL and thus no fluorescent signal is observed. In the presence of the target DNA sequence, the loop section in MBs can hybridize with their complementary target DNA. Since the hybridization between the loop section and the target is stronger than the stem section

alone, the MBs undergo conformational change and thus the fluorophores and quencher molecules are separated from each other. As a result, a fluorescent signal is observed.

Until now, MBs have been applied in various applications including real-time monitoring of polymerase chain reactions [1,2], developing DNA sensors [3], and in monitoring target RNAs in vivo for drug development [4]. As nucleic acid probes, MBs do not require washing step and their hairpin structure offers high specificity, and thus enables to discriminate single mismatched target molecules. Since the first appearance of MBs in 1996, MBs have been continuously improved and new types of MBs have been developed including surface immobilized [5,6], wavelength-shifted [7], nano gold-quenched [8], and multicolor MBs [9]. However, for practical in vivo application of MBs, their limitation still remains due to the photobleaching characteristics of the organic dyes and their available limited number of colors [9]. Since the life time of organic dyes is not long enough, it is challenging in applications such as the observation of the expression of target RNA in vivo. Furthermore, organic dyes have their own excitation wavelength that results in a serial imaging processing for different colored organic dyes during multiplexed imaging which can cause energy accumulation in living cells. Since most of the time their spectra

\* Corresponding author. Tel.: +1 909 787 2900; fax: +1 909 787 2425.  
E-mail address: [mihri@ee.ucr.edu](mailto:mihri@ee.ucr.edu) (M. Ozkan).

overlap, it is difficult to observe two different colors at the same time and this can limit the number of detectable targets. To overcome these limitations, here we present a new engineered QD-conjugated MBs.

In these new probes, MB's organic fluorophores are replaced with inorganic and semiconducting QDs (Fig. 1). Semiconducting QDs have been used for various applications in molecular and cellular biology [10,11]. Recently developed mono-dispersed QDs have substantial advantages over organic dyes: tunable colors by changing the particle size, a single wavelength for simultaneous excitation of different-sized QDs, high stability against photobleaching, narrow and symmetrical emission peaks [12–14]. Due to the better photostability characteristics of QDs, to enable longer imaging both in vitro and in vivo applications, we choose to replace the organic fluorophores of the conventional MB with QD. Here, we explain synthesis of these hybrid MBs and their FRET efficiency analysis as compared to the commercial MBs.

## 2. Materials and methods

### 2.1. Synthesis of QD-modified molecular beacons

0.5 ml of ZnS-capped CdSe QDs (3.7 nm in diameter) purchased from Evident Technologies (Troy, NY) in a toluene solution were reacted with  $\sim 1.0$  M mercaptoacetic acid (MAA) for at least 2 h. During the reaction, QDs were precipitated by the exchange of tri-*n*-octylphosphine oxide (TOPO) with MAA. The MAA-capped QDs were purified by centrifugation and washed with equal volume of chloroform five times. Later, the chloroform was removed by evaporation at room temperature over a minimum period of 2 h. Finally, the modified QDs were re-suspended in 0.5 ml phosphate-buffered saline (PBS) solution (pH 7.4).

### 2.2. Target DNA attachment

Ten microliters of modified QDs were conjugated with  $\sim 1$   $\mu$ M of 25 base MB (5'(C<sub>6</sub>NH<sub>2</sub>) GCGACTTTG-

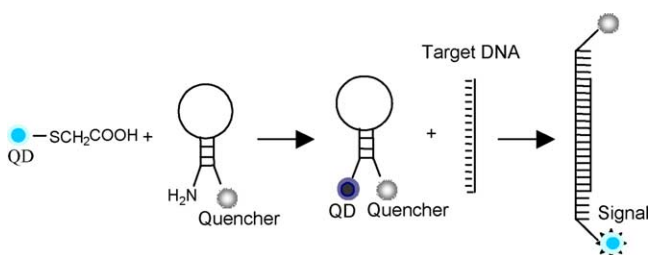


Fig. 1. Schematic illustration of making of quantum dot (QD)-modified molecular beacons. Surface functionalized QDs are conjugated with amine terminated MBs at 5' end. At the "off" state (closed) of MB, there is no signal and after addition of target DNA sequence, MB opens. Since QD and quencher are separated from each other, QD's emission can be detected.

GGTTTGGGTTTCTCGC (DABCYL)-3') obtained from Midland Certified Reagent Company (Midland, TX) in 980  $\mu$ l PBS, pH 8.2 for 24 h at room temperature. For this reaction, EDC (1-ethyl-3-(3-dimethylaminopropyl)carbodiimide hydrochloride) agent (10-fold mole more than MB) was used. Hybridization between the QD-conjugated MBs (1  $\mu$ M) and their target molecules occurred in a solution containing 20 mM Tris-HCl, 50 mM KCl, and 5 mM MgCl<sub>2</sub> at pH 8. During the experiment, first background signal of 800  $\mu$ l PBS solution was measured by using SIMADZU RF-551 spectrofluorometer. One hundred microliters of the sample containing the QD-conjugated MBs (1  $\mu$ M) was then added into the solution. After measuring the intensity of fluorescence in the sample, the fluorescence of MBs with 10-fold molar excess perfect matched base pairs were detected.

### 2.3. Molecular modeling

For comparison of the organic-based MBs with QD-MBs, 3-D molecular modeling of these structures was performed. In order to accomplish this, the Biopolymers module of Insight II (Accelrys, Inc., San Diego) was used. Here, the 25 base DNA loop that forms the molecular beacon, QD connected through the amide bond to the 5' end of the molecular beacon and for a quencher chain containing DABCYL connected to the 3' end of the molecular beacon, with their respective chemistries, was modeled. Similarly, 6-Fam attached (5' end) 25 base DNA together with DABCYL connected at 3' end was also modeled to predict the potential nearest and farthest distances between the 6-Fam and DABCYL. Four base pairs were constrained to form a B-DNA structure for the MB stem. The remainder of the structure was subjected to several rounds of energy minimization and molecular dynamics runs to relax the MB loop structure, using the Discover module of Insight and the AMBER force field. The QD is represented by a sphere with diameter of 3.7 nm, and was modeled as a pseudo-atom with van der Waals radius of 1.85 nm, located at an arbitrary position that accounts for the sum of the van der Waals radii of the terminal sulfur-pseudo-atom pair.

### 2.4. Calculation of FRET efficiency

According to Förster's theory, quenching or FRET efficiency,  $E$ , is given by [15],

$$E = \frac{R_0^6}{R_0^6 + R^6} \quad (1)$$

where,  $R_0$  is Förster radius, the distance at which transfer efficiency is 50%, and  $R$  is the distance between the centers of the fluorophore and acceptor. Förster radius is given as,

$$R_0 = (8.8 \times 10^{23} JK^2 Q_0 n^{-4})^{1/6} \text{ \AA} \quad (2)$$

where,  $K^2$  is the orientation factor for a dipole-dipole interaction,  $J$  is the spectral overlap integral in  $M^{-1} \text{ cm}^3$ ,  $Q_0$  is

the quantum yield of donor without acceptor, and  $n$  is the refractive index of the medium between the donor and acceptor [15]. Based on our calculation, the overlap integral of QD and 6-Fam are  $1.32 \times 10^{-13}$  and  $6.23 \times 10^{-14}$ , respectively (for this calculation,  $K^2 = 2/3$  for random orientation, and  $n = 1.33$ ). For 6-FAM, since its structure looks very similar to 5-FAM, the quantum yield for 5-FAM at pH 8.0 that is published in the reference [16] was used to calculate the Förster radius. In addition, the quantum yield of the modified QD is estimated as 6.8% by comparison with fluorescein whose quantum yield is 0.92 in 0.1N NaOH. [17]

### 3. Results and discussion

#### 3.1. Absorption and emission spectra of MAA functionalized QD

For characterization, the spectrum of absorbance and excitation of the modified QDs with MAA monolayer are compared to TOPO-capped QDs (Fig. 2). The maximum absorbance of TOPO-capped QDs and MAA monolayer-capped QDs occurred at 462 and 461 nm, respectively. The difference is within the repeatability range of the spectrophotometer. In the case of emission, QDs have a symmetric Gaussian spectrum, even though a slight red shift of the maximum emission peak from 483 to 489 nm was observed after surface functionalization. In both cases, full width at half maximum (FWHM) remains at 37 nm. This FWHM is slightly higher than the reported values [12–14]. We believe that these QDs were slightly larger than the average of 3.7 nm in size and their size distribution was about 5% as we confirmed with Evidot Technologies. A shift to-

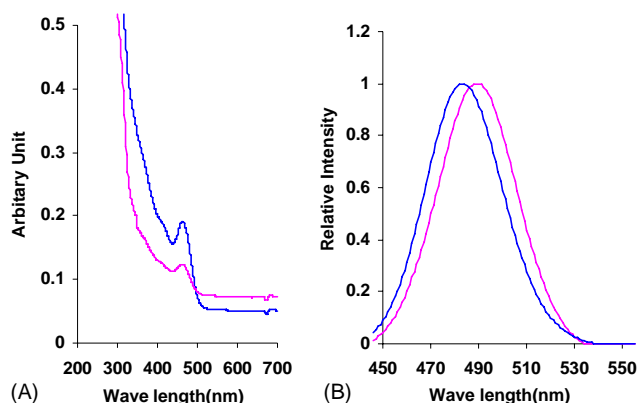


Fig. 2. Spectrum of QD with 3.7 nm in diameter using in our experiments. (A) Absorption, and (B) emission before (blue) and after (red) surface functionalization with MAA. The slight red shift in the spectrum is within the repeatability limit of the spectrofluorometer used during the measurements. Notice slightly broader bandwidth compared to the QDs in the figure. The size distribution in these QDs is found in the range of 5%. (For interpretation of the references to color in this figure legend, the reader is referred to the web version of this article.)

wards the red in the emission spectrum can be due to the increase in the final size of the QD after surface functionalization. However, compared to the conventional organic fluorophores (FWHM is  $\sim 50$  nm), our QDs have a very narrow FWHM. When QD and DABCYL are within close proximity to each other and the emission spectrum of QD can overlap with the absorption spectrum of DABCYL, energy can be transferred from the QD to the DABCYL and thus absorbed energy dissipates as heat. To verify whether DABCYL can be used as a quencher molecule for QD-modified MBs, the emission spectrum of the QDs with MAA monolayer was compared with the absorption spectrum of DABCYL. About 90% overlap was observed (not shown here). For the case of 6-Fam the overlap was less than 30%.

#### 3.2. FRET efficiency of 6-Fam/DABCYL and QD/DABCYL

Fig. 3 depicts the snap shots from the molecular modeling of QD/DABCYL MB and 6-Fam/DABCYL organic MB. We choose 6-Fam (organic dye) for comparison just because it had the most similar emission spectrum like our blue QD as compared to other organic dyes we have tested. The QD in this model was 3.7 nm in size and attached to 5' end of the MB. The 3' end had DABCYL as an organic quencher. It should be noted that molecular beacon is capable of spanning a large conformational space, mediated by the multiple rotameric states of the aliphatic thiol linker of the QD and the linker of DABCYL and by the typical flexibility of DNA molecule. Especially inside a buffer solution, spatial distribution can change dynamically and thus the distance between the donor (6-FAM or QD) and acceptor (DABCYL). As a consequence, as can be observed from Eq. (1), this could affect the FRET efficiency between 6-FAM/DABCYL and QD/DABCYL.

As Fig. 3A and B illustrates, the potential nearest and farthest distance between QD and DABCYL are predicted as 3.3 and 5 nm, respectively. For the distance measurements, the distance from the center of the QD to the N=N bond of DABCYL (taken as the center of DABCYL) is measured. By using the Eq. (2), Förster radius [1–3,16] is calculated as 3.4 nm for modified QD/DABCYL MB. Finally, the corresponding FRET efficiency for Fig. 3A and B is calculated to be  $\sim 54$  and  $\sim 9\%$ , respectively. As comparison, Fig. 3C and D demonstrate relative distances between 6-FAM and DABCYL to be 2.4 and 3.4 nm. For the distance measurements, the distance from the C9 in Xanthene of 6-FAM (taken as the center of 6-FAM) to the N=N bond of DABCYL (taken as the center of DABCYL) is measured. Förster radius is calculated as 4.6 nm using Eq. (2). Eq. (1) gives FRET efficiency to be 98% (Fig. 3C) and 87% (Fig. 3D). As a conclusion, due to the larger size of the QD the center-to-center spacing between QD and DABCYL is found to be larger as compared to the 6-FAM/DABCYL case. This affects the efficiency of FRET negatively. Similarly, the Förster radius of QD/DABCYL

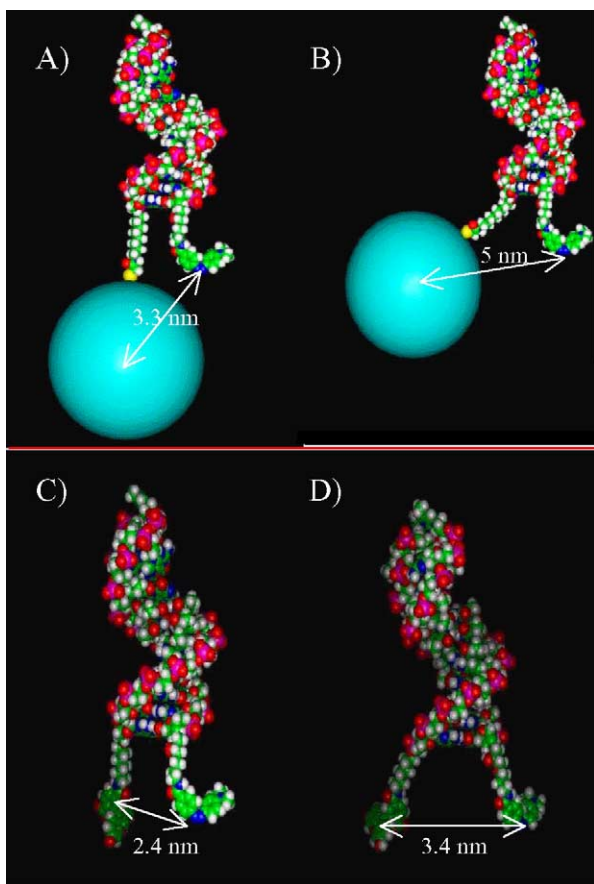


Fig. 3. 3-D molecular modeling of QD-modified MBs. This model is a snap shot of a highly dynamic macromolecule. Size of QD here is 3.7 nm. (A) The nearest possible separation between QD and DABCYL, (B) the farthest possible separation between QD and DABCYL, (C) the nearest possible separation between the 6-FAM and DABCYL, (D) the farthest separation between the 6-FAM and DABCYL. The color code for elements is as follows: red: oxygen; green: carbon; pink: phosphorus; white: hydrogen; blue: nitrogen; lake blue: quantum dot. (For interpretation of the references to color in this figure legend, the reader is referred to the web version of this article.)

(3.4 nm) is smaller than the 6-FAM/DABCYL (4.6 nm). This also affects the final FRET efficiency negatively. However, the overlap integral between the QD/DABCYL is much higher as compared to the 6-FAM/DABCYL. Hence due to the compound effect FRET efficiency for QD/DABCYL MB is predicted less than 6-FAM/DABCYL MB. At the end, the FRET efficiency of QD/DABCYL is calculated to be smaller as compared to 6-FAM/DABCYL. However, in our experiments, the increase in fluorescence was found sufficient enough for the detection purposes. For our future experiments, we would like to use a better filtration method that can separate our unconjugated QDs from conjugated QD/MBs. As a result the final increase in the emission after the addition of the target might be better than the results presented here. The advantageous characteristic of QD/DABCYL MB is found to be their stability against photobleaching. About 15% decrease in the fluorescence was

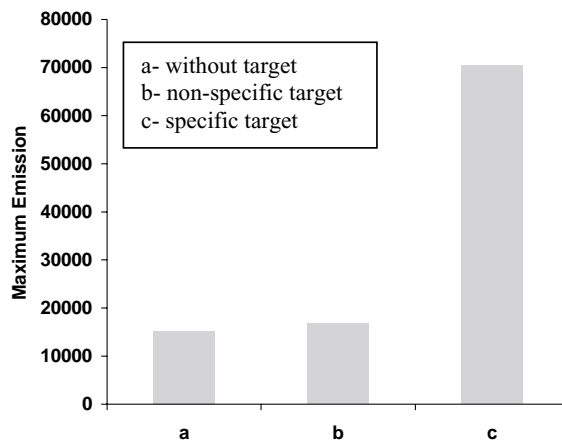


Fig. 4. Specificity of QD MBs for their targets. After the addition of complementary target sequence the fluorescence signal increased about five-fold, while the signal did not change for the non-specific target addition.

observed with 6-FAM MBs while the fluorescence of QD MBs remained constant over 10 min of continues excitation.

### 3.3. Performance of QD-conjugated MB

Fig. 4 depicts the performance of QD MBs. As shown in the figure the fluorescence increased with the addition of the complementary target DNA sequence, while no increase in the fluorescence is observed after the addition of the non-specific target sequence. In the later case, the signal remained similar to the baseline fluorescence measured prior to the addition of the any target sequences. This result depicts the specificity of QD MBs. Even though in average about six-fold of increase in the fluorescence after the addition of the target sequence is observed with QD/DABCYL (in average this is about to be 10-fold for organic-based MBs), the stability in the signal can offer long-term analysis with the QD MBs.

## 4. Conclusions

We have developed new hybrid quantum dot-conjugated molecular beacons. With perfectly matched target oligonucleotides, the signal to background ratio was about 5–6. Although some improvements are desired regarding the relatively low signal to background ratio as compared to organic counterparts, our work demonstrates improved lifetime during the imaging as compared to the organic MBs. As reported, the nanocrystals have substantial advantages over organic dyes such as tunable colors by changing the particle size, a single wavelength for simultaneous excitation of different-sized QDs, high stability against photobleaching, and narrow and symmetrical emission peaks. This could, in the future, enable simultaneous multiplexed DNA or RNA detection in vivo and can offer great advances in genomics and medicine.

## Acknowledgments

We thank to the University of California, Riverside for supporting this research.

## References

- [1] S. Tyagi, F.R. Kramer, Molecular beacons: probes that fluoresce upon hybridization, *Nat. Biotechnol.* 14 (1996) 303–308.
- [2] D.L. Sokol, X. Zhang, P. Lu, A.M. Gewirtz, Real time detection of DNA-RNA hybridization in living cells, *Proc. Natl. Acad. Sci. U.S.A.* 95 (1998) 11538–11543.
- [3] X. Liu, W. Farmerie, S. Schuster, W. Tan, Molecular beacons for DNA biosensors with micrometer to submicrometer dimensions, *Anal. Biochem.* 15 (1999) 56–63.
- [4] T. Matsuo, In situ visualization of messenger RNA for basic fibroblast growth factor in living cells, *Biochim. Biophys. Acta* 1379 (1998) 178–184.
- [5] W. Tan, X. Fang, J. Li, X. Liu, Molecular beacons: a novel DNA probe for nucleic acid and protein studies, *Chem. Eur. J.* 6 (2000) 1107–1111.
- [6] X. Fang, X. Liu, S. Schuster, W. Tan, Designing a novel molecular beacon for surface-immobilized DNA hybridization studies, *J. Am. Chem. Soc.* 121 (1999) 2921.
- [7] S. Tyagi, S.A.E. Marrs, R. Kramer, Wavelength-shifting molecular beacons, *Nat. Biotechnol.* 18 (2000) 1191–1196.
- [8] B. Dubertret, M. Calame, A.J. Libchaber, Single-mismatch detection using gold-quenched fluorescent oligonucleotides, *Nat. Biotechnol.* 19 (2001) 365–370.
- [9] S. Tyagi, D.P. Bratu, F.R. Kramer, Multicolor molecular beacons for allele discrimination, *Nat. Biotechnol.* 16 (1998) 49–53.
- [10] M. Dahan, T. Laurence, F. Pinaud, D.S. Chemla, A.P. Alivisatos, M. Sauer, S. Weiss, Time-gated biological imaging by use of colloidal quantum dots, *Opt. Lett.* 26 (2001) 825–827.
- [11] D.M. Willard, L.L. Carillo, J. Jung, A. Van Orden, CdSe-ZnS quantum dots as resonance energy transfer donors in a model protein-protein binding assay, *Nano Lett.* 1 (2001) 467–474.
- [12] W. Chan, N. Shuming, Quantum dot bioconjugates for ultrasensitive nonisotopic detection, *Science* 281 (1998) 2016–2018.
- [13] M. Bruchez Jr., M. Moronne, P. Gin, S. Weiss, A.P. Alivisatos, Semiconductor nanocrystals as fluorescent biological labels, *Science* 281 (1998) 2013–2016.
- [14] P. Alivisatos, Semiconductor clusters, nanocrystals, and quantum dots, *Science* 271 (1996) 933–937.
- [15] M. Nirmal, L.E. Brus, Luminescence photophysics in semiconductor nanocrystals, *Acc. Chem. Res.* 32 (1999) 407–414.
- [16] J. Ju, C. Ruan, C.W. Fuller, A.N. Glazer, R.A. Mathies, Fluorescence energy transfer dye-labeled primers for DNA sequencing and analysis, *Proc. Natl. Acad. Sci. U.S.A.* 92 (1995) 4347–4351.
- [17] T. Ratilainen, A. Holmén, E. Tuite, G. Haaima, Leif. Christensen, P.E. Nielsen, B. Nordén, Hybridization of peptide nucleic acid, *Biochemistry* 37 (1998) 12331–12342.